JOURNAL OF GUIDANCE, CONTROL, AND DYNAMICS
Vol. 17, No. 6, November–December 1994

Analytical Aeropropulsive/Aeroelastic Hypersonic-Vehicle Model with Dynamic Analysis

Frank R. Chavez* and David K. Schmidt†
University of Maryland at College Park, College Park, Maryland 20742

The determination of the dynamic characteristics of hypersonic vehicles requires an integrated approach since the propulsion system and airframe are so highly coupled. The forces and moments arise from both aerodynamic and propulsive sources, which are for these configurations hard to separate. Offered herein is a first step toward the development of such an approach that is intentionally generic and basic. Further, analytical expressions are developed to allow for characterization of the vehicle's dynamics early in the design cycle, so that configuration trade-offs may be performed with some cognizance of the attitude dynamics. The method of approach involves a two-dimensional hypersonic aerodynamic analysis utilizing Newtonian theory, coupled with a one-dimensional aero/thermo analysis of the flow in a SCRAMjet-type propulsion system. In addition, the airframe is considered to be elastic, and the structural dynamics are characterized in terms of a simple lumped-mass model of the in vacuo vibration modes. The vibration modes are coupled to the rigid-body modes through the aero/propulsive forces acting on the structure. The control effectors considered on a generic study configuration include aerodynamic pitch-control surfaces as well as engine fuel flow and diffuser area ratio. It is shown that the vehicle's aerodynamics and propulsive forces are both very significant in the evaluation of key stability derivatives that dictate the vehicle's dynamic characteristics. It is also shown that the vehicle model selected is highly unstable in pitch and exhibits strong airframe/engine/elastic coupling in the aeroelastic and attitude dynamics. With the use of literal expressions for both the system's poles and zeros as well as the stability derivatives, key vehicle dynamic characteristics are investigated. For small errors, or uncertainties, in either the aerodynamic or propulsive forces, significant errors in the frequency and damping of the dominant modes and zero locations will arise.

Nomenclature

$\bar{A}_D$	= diffuser area ratio
$\bar{A}_N$	= internal nozzle area ratio
b	= vehicle width parameter
C_p	= pressure coefficient, $(P - P_\infty)/(\frac{1}{2}\rho_\infty V_\infty^2)$
g	= acceleration due to gravity
h	= vehicle height
I_1	= $[(\bar{P} - 1) - \ln(\bar{P})]/(\bar{P} - 1)^2$
I_2	= $[(\bar{P} + 1)\ln(\bar{P}) - 2(\bar{P} - 1)]/(\bar{P} - 1)^3$
I_{yy}	= vehicle y axis inertia per unit width
L	= vehicle length
L_1	= distance from vehicle nose to apex
L_2	= distance from vehicle tail to apex
l_1	= lower fore-body surface length, $L_1/\cos\tau_1$
l_2	= lower aft-body surface length, $L_2/\cos\tau_2$
M	= total moment about mass center
M_{cs}	= moment due to control surface
m	= vehicle mass per unit width
$\mathfrak{m}$	= generalized elastic mass per unit width
$P_1(s_1)$	= pressure along lower fore-body
$P_2(s_2)$	= pressure along lower aft-body
$P_u(s_u)$	= pressure along upper surface
$\bar{P}$	= pressure ratio, P_e/P_∞
Q	= total generalized elastic force
q	= vehicle rigid-body pitch rate
q_∞	= dynamic pressure, $\frac{1}{2}\gamma M_\infty^2 P_\infty$
S_{cs}	= control surface reference area
T_0	= total temperature across combustor
Th	= thrust per unit width of vehicle
v	= local flow velocity vector
X	= total force along vehicle x axis
X_{cs}	= x-axis force due to control surface
$\bar{x}$	= x distance to vehicle mass center
x_{cs}	= x control surface position
Z	= total force along vehicle z axis
Z_{cs}	= z-axis force due to control surface
$\bar{z}$	= z distance to vehicle mass center
z_{cs}	= z control surface position
$[A]$	= aerodynamic stability derivatives
$[A_c]$	= aerodynamic control derivatives
$[E]$	= external nozzle stability derivatives
$[E_c]$	= external nozzle control derivatives
$[\bar{E}]$	= engine sensitivities
$[\bar{E}_c]$	= engine control sensitivities
$[F]$	= engine thrust sensitivities
$[F_c]$	= engine thrust control sensitivities
$[T]$	= engine thrust stability derivatives
$[T_c]$	= engine thrust control derivatives
α	= angle of attack
$\begin{Bmatrix} \Delta\tau_1 \\ \Delta\tau_1 \end{Bmatrix}$	= elastic mode shape
δ	= control surface deflection
γ	= ratio of specific heats
η	= generalized elastic coordinate
ω_1	= natural frequency of first in vacuo vibration mode
τ_n	= vehicle nose angle
τ_t	= vehicle tail angle
$\theta_L(s_1)$	= local-flow deflection angle
θ_L	= nominal-flow deflection angle
ζ_1	= damping ratio of first in vacuo vibration mode

Subscripts

A	= due to aerodynamics
E	= due to external nozzle
e	= internal nozzle/engine exit conditions
T	= due to engine thrust
0	= trim condition

Presented as Paper 92-4567 at the AIAA Atmospheric Flight Mechanics Conference, Hilton Head, SC, Aug. 10–12, 1992; received Oct. 31, 1992; revision received Feb. 1, 1994; accepted for publication Feb. 23, 1994.

*Doctoral Student, Department of Aerospace Engineering. Student Member AIAA.

†Professor and Chairman, Department of Aerospace Engineering. Associate Fellow AIAA.

1 = engine/diffuser inlet conditions
2 = combustor inlet conditions
3 = internal nozzle inlet conditions
∞ = freestream conditions

Introduction

HYPERSONIC vehicles promise to be among the greatest technological challenges ever taken on by the international aerospace community. As discussed in Refs. 1–3, for example, their dynamics are strongly dependent on both aerodynamic and propulsive effects, and these are in fact difficult to separate. Hence, an integrated modeling approach is required. Specifically, since the entire undersurface of the vehicle is part of the inlet and the nozzle of the propulsion system, a significant amount of "propulsive lift" will be generated, along with "propulsive moments" acting on the vehicle, both of which will vary with the propulsive thrust being produced. Furthermore, the structure is elastic; therefore, elastic deformations of the fore-body as well as vehicle pitch response will affect the propulsion system's inlet conditions, which in turn will introduce disturbances propagating through the engine and back into the airframe/nozzle.

Although the methodology presented here integrates all the aforementioned features into the modeling, it is also intentionally kept conceptually simple so that analytical expressions may be obtained for key results. This is in contrast to a purely numerical method, which will ultimately be required for more detailed analysis of a specific vehicular configuration. The basic approach taken here is intended to be useful early in the design cycle, during configuration definition, in order to identify critical configuration-dependent dynamics-and-control issues early and to develop a basic understanding of the physical genesis of these control issues.

In this paper, such an integrated modeling approach is developed and applied to the characterization of a generic hypersonic vehicle configuration. Two-dimensional Newtonian theory is utilized to characterize the aerodynamic pressure distribution on the fore-body, whereas two-dimensional shock expansion theory is used to determine the pressure distribution on the afterbody/nozzle. A one-dimensional aero/thermo/gasdynamic model is employed to characterize the flow in a SCRAMjet-type engine. Finally, a lumped-mass dynamic model is employed to characterize the structure's vibration characteristics. The shape-dependent pressure distributions are then integrated and the expressions for the forces and moments are linearized to allow for analysis of the attitude dynamics. As noted above, analytical expressions for the stability derivatives, as well as numerical results, will be developed and the significance of the vehicle's aerodynamic and propulsive forces are quantified with respect to both the stability derivatives and to the vehicles' dynamics.

Although the methods used herein are intentionally simple, sufficient validity is certainly required. In this regard, the following points and comparisons are in order. As shown by Maughmer et al.,[4] the Newtonian method gives surprisingly good estimates for forces and moments. Although more complex aerodynamic prediction methods are required for estimating heat transfer, for example, this is not the problem addressed here. As with any aeroelastic analysis, the accuracy of the structural dynamics model depends directly on the accuracy of the predicted mode shapes and vibration frequencies. Since the mode shape and vibration frequency used here are based on a complete NASTRAN analysis[5] of a vehicle with similar geometry, this aspect of the structural model is assumed adequate. As for the propulsion model, pressures and Mach numbers in the engine at various stations are very close to those presented by Baranovsky et al.[6] and hence appear to be reasonable. Finally, it will be shown that the study-vehicle configuration considered in this paper is statically unstable, which agrees with the analysis of a similar vehicle by Cheng.[7]

A Generic Hypersonic Vehicle Configuration

The X-30 configuration, taken from Ref. 8, is shown in Fig. 1. Specifically, note the side view of the hypersonic vehicle. The vehicle's lower fore-body surface serves two purposes: The first is to produce "lift" and the second is to act as an external diffuser to slow the flow velocity and increase the pressure at the inlet to the engine. The vehicle's afterbody/nozzle surface serves as an external expansion nozzle to produce thrust and also lift. The upper surface is basically flat and contributes little to the aerodynamics of the vehicle compared to the effects of the lower surfaces.

Figure 2 illustrates the two-dimensional model of a generic hypersonic vehicle to be used for the analysis of this class of vehicle. The two-dimensional model incorporates two key characteristics of the hypersonic vehicle, a fore-body compression surface and an afterbody/nozzle expansion surface; yet the geometry is intentionally kept simple.

The elastic motion of the vehicle is characterized by a single body-bending mode, as shown in Fig. 3. The primary effect of this elastic deformation is to change the effective "slope" of the lower fore-body and afterbody/nozzle surfaces. Again, the characterization of the elastic motion of the vehicle is kept simple to aide in the analysis yet still retain first-order effects.

The SCRAMjet engine module consists of three main sections, a supersonic diffuser, a supersonic combustor, and an internal supersonic expansion nozzle, as shown in Fig. 4. The inlet conditions to the engine are determined by the aerodynamics associated with the lower fore-body surface of the vehicle, whereas the exit conditions of the engine will strongly affect the pressure distribution over the vehicle's afterbody/nozzle surface. Finally, the engine is considered to have a variable diffuser area ratio and a variable fuel flow rate.

Forces and Moments

The pressures over the surface of the vehicle give rise to forces and moments about the mass center and to generalized forces associated with the interaction between these pressures and the elastic motion of the vehicle. As indicated in Fig. 2, there are two distinct flow regions surrounding the vehicle. The first, region I, is essentially the freestream over the vehicle's upper and lower fore-body surfaces and the aerodynamic pitch-control surfaces. The second

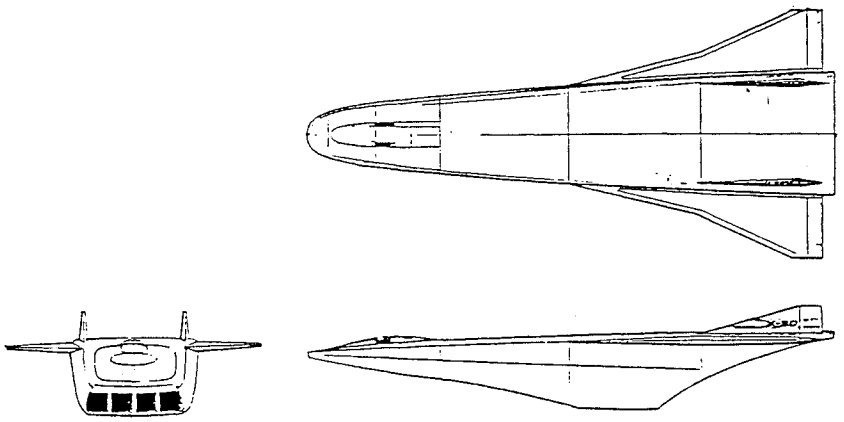

Fig. 1 X-30 configuration.[8]

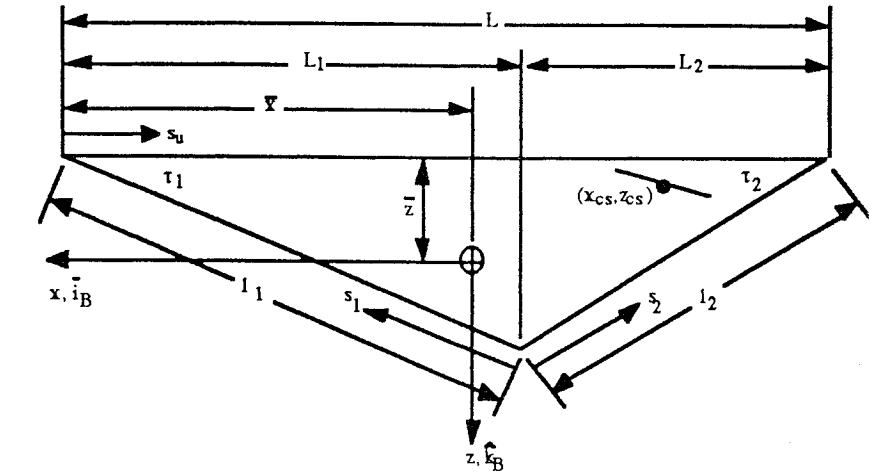

a) Vehicle geometry

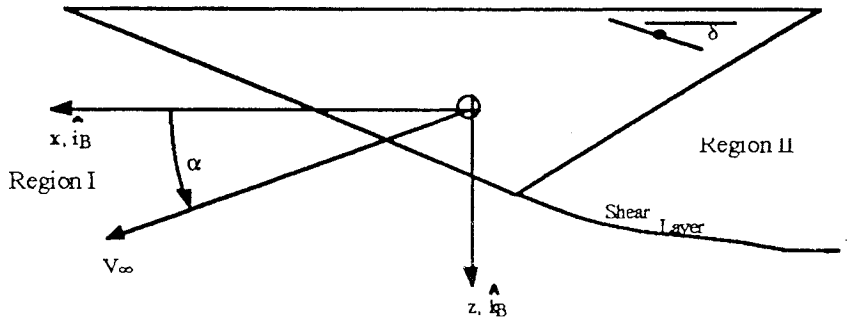

b) Flow regions

Fig. 2 Two-dimensional vehicle geometry.

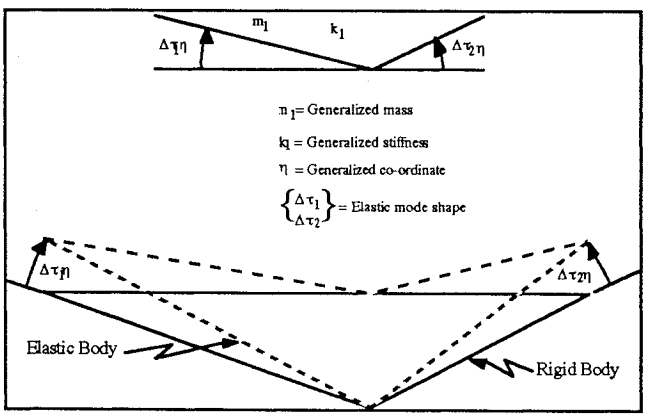

Fig. 3 Elastic vehicle model.

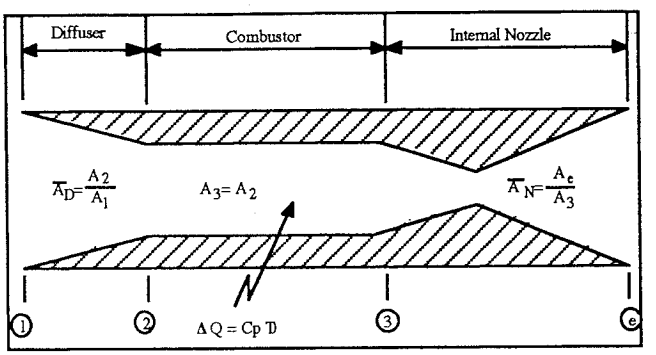

Fig. 4 Engine module.

flow region, region II, gives rise to a pressure distribution along the vehicle's afterbody/nozzle surface and is due to both the vehicle's engine exhaust plume and the interaction between the plume and the freestream. Hence, a combined gasdynamic/thermodynamic and aerodynamic analysis will be needed for determining the pressure in this region. The thrust developed by the engine module also gives rise to moments about the mass center. Therefore, the forces and moments, along with the generalized elastic forces, can be separated into three components. The three components will be referred to as the aerodynamic, denoted by a subscript A, the engine's thrust, denoted by a subscript T, and the engine's exhaust gas, denoted by a subscript E.

Let the expressions for the force and moment per unit vehicle width be expressed in vector form as

$$F = X\hat{i}_B + Z\hat{k}_B \tag{1}$$

$$M = M\hat{j}_B \tag{2}$$

where $\hat{i}_B$, $\hat{j}_B$, and $\hat{k}_B$ are unit vectors along the x, y, and z axes of the vehicle reference frame, shown in Fig. 2, which has origin at the vehicle's instantaneous mass center. Also, X is the force along the x axis, Z is the force along the z axis, and M is the pitching moment about the y axis.

The above forces and moment can be expressed in terms of the three components arising from the aerodynamics, the engine thrust, and the engine exhaust gas mentioned above as

$$X = X_A + X_T + X_E \tag{3}$$

$$Z = Z_A + Z_T + Z_E \tag{4}$$

$$M = M_A + M_T + M_E \tag{5}$$

The generalized force associated with the elastic degree of freedom of the vehicle can be obtained from the virtual work δW.[9,10] In terms of the components due to the effects of the aerodynamics, the

engine thrust, and the engine exhaust gas, this generalized force will be expressed as

$$\frac{\delta(\delta W)}{\delta \eta} = Q = Q_A + Q_T + Q_E \tag{6}$$

Aerodynamic Analysis

If the flow in region I is assumed to be two-dimensional and inviscid, then the pressure on the lower fore-body surface of the vehicle is simply the pressure on an inclined surface in supersonic flow,[9] which is given by oblique shock theory.[11] An approximation to this theory for large Mach numbers (i.e., hypersonic flow) is given by Newtonian impact theory[11–13] with pressure, temperature, and Mach number given as

$$P_1(s_1) = P_\infty\left[1 + \tfrac{1}{2}\gamma M_\infty^2 C_{p_N} \sin^2\theta_L(s_1)\right] \tag{7}$$

$$T_1(s_1) = T_\infty\left[1 + \tfrac{1}{2}(\gamma - 1)M_\infty^2 \sin^2\theta_L(s_1)\right] \tag{8}$$

$$M_1(s_1) = \frac{M_\infty \cos\theta_L(s_1)}{\sqrt{1 + \tfrac{1}{2}(\gamma - 1)M_\infty^2 \sin^2\theta_L(s_1)}} \tag{9}$$

where the pressure coefficient $C_{p_N} = 2$, s_1 is the distance from the vehicle's lower apex to the point of interest, as shown in Fig. 2, and $\theta_L(s_1)$ is the local flow deflection angle, which can be expressed in terms of the local flow velocity vector and the local outward normal vector, as shown in Fig. 5.

The pressure on the vehicle's upper surface, P_u, is just the pressure on an expansion surface in hypersonic flow. For small expansion angles, assumed here, the approximation $P_u = P_\infty$ is made.

Integrating Eq. (7) along the lower fore-body, the forces and moment due to the aerodynamics are given by[9]

$$X_A = -\left[P_\infty l_1 + q_\infty C_{p_N}\int_0^{l_1} \sin^2\theta_L(s_1)\,ds_1\right] \times \sin(\tau_1 + \Delta\tau_1\eta) + X_{cs} \tag{10a}$$

$$Z_A = P_\infty L - \left[P_\infty l_1 + q_\infty C_{p_N}\int_0^{l_1} \sin^2\theta_L(s_1)\,ds_1\right] \times \cos(\tau_1 + \Delta\tau_1\eta) + Z_{cs} \tag{11a}$$

$$M_A = \left[\tfrac{1}{2}P_\infty l_1^2 + q_\infty C_{p_N}\int_0^{l_1} s_1 \sin^2\theta_L(s_1)\,ds_1\right] [(h - \bar{z})\sin(\tau_1 + \Delta\tau_1\eta) + (L_1 - \bar{x})\cos(\tau_1 + \Delta\tau_1\eta)] \times \left[P_\infty l_1 + q_\infty C_{p_N}\int_0^{l_1} \sin^2\theta_L(s_1)\,ds_1\right] - P_\infty L\left(\bar{x} - \tfrac{1}{2}L\right) + M_{cs} \tag{12a}$$

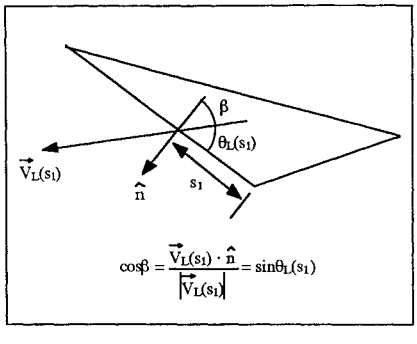

Fig. 5 Geometry for local flow deflection angle.

$$Q_A = \Delta\tau_1\left[\tfrac{1}{2}P_\infty l_1^2 + q_\infty C_{p_N}\int_0^{l_1} s_1 \sin^2\theta_L(s_1)\,ds_1\right] \tag{13}$$

The expressions for the forces and moment due to the control surface are also determined using Newtonian theory and are given by[9]

$$X_{cs} = -q_\infty C_{p_N}\sin^2(\alpha + \delta)\sin\delta(S_{cs}/b) \tag{10b}$$

$$Z_{cs} = -q_\infty C_{p_N}\sin^2(\alpha + \delta)\cos\delta(S_{cs}/b) \tag{11b}$$

$$M_{cs} = X_{cs}z_{cs} - Z_{cs}x_{cs} \tag{12b}$$

where (x_{cs}, z_{cs}) is the position of the control surface relative to the vehicle's mass center.

Given these expressions for the forces and moment acting on the vehicle, the stability derivatives can be obtained from linearization of the above expressions by expanding them into a first-order Taylor series about some nominal, or trim, condition of the vehicle. The stability derivatives are then the coefficients of the perturbation motion quantities. The perturbation quantities to be used here are the freestream Mach number M_∞, the angle of attack α, the pitch rate q, and the elastic degree of freedom η and rate $\dot{\eta}$. Here, the angle of attack and pitch rate are defined in terms of the vehicle coordinate frame.

Let the set of linearized equations for the perturbation aerodynamic forces and moment, expressed in terms of the aerodynamic stability derivatives and the aerodynamic control derivatives, be expressed in matrix form as[9]

$$\begin{Bmatrix} \Delta X_A \\ \Delta Z_A \\ \Delta M_A \\ \Delta Q_A \end{Bmatrix} = [A]\begin{Bmatrix} \Delta M_\infty \\ \Delta\alpha \\ \Delta q \\ \Delta\eta \\ \Delta\dot{\eta} \end{Bmatrix} + [A_c]\{\Delta\delta\} \tag{14}$$

where

$$[A] = \begin{bmatrix} (X_A)_{M_\infty} & (X_A)_\alpha & (X_A)_q & (X_A)_\eta & (X_A)_{\dot{\eta}} \\ (Z_A)_{M_\infty} & (Z_A)_\alpha & (Z_A)_q & (Z_A)_\eta & (Z_A)_{\dot{\eta}} \\ (M_A)_{M_\infty} & (M_A)_\alpha & (M_A)_q & (M_A)_\eta & (M_A)_{\dot{\eta}} \\ (Q_A)_{M_\infty} & (Q_A)_\alpha & (Q_A)_q & (Q_A)_\eta & (Q_A)_{\dot{\eta}} \end{bmatrix} \tag{15}$$

$$[A_c] = \begin{bmatrix} (X_A)_\delta \\ (Z_A)_\delta \\ (M_A)_\delta \\ (Q_A)_\delta \end{bmatrix} \tag{16}$$

The subscript in the above matrices refers to the partial derivative with respect to that quantity. Taking the partial derivatives of the aerodynamic forces and moment [Eqs. (10–13)] with respect to the perturbation quantities, the aerodynamic stability and control derivatives can be obtained in closed form.[9] The aerodynamic stability derivatives and the aerodynamic control derivatives are listed in Table 1.

Engine Analysis

The engine module consists of three sections, as shown in Fig. 4. An isentropic, quasi-one-dimensional assumption is made for the flow in both the diffuser and the internal nozzle, whereas the flow in the combustion chamber is characterized as quasi-one-dimensional in a constant area duct with heat addition. This heat addition, due to the combustion of the fuel, gives rise to an increase in the total temperature across the combustor, denoted herein by T_0. The working fluid is assumed to be a perfect gas with constant specific heats.

The inlet conditions to the diffuser, which are the inlet conditions to the engine module, must be determined from the aerodynamic analysis of the vehicle's lower fore-body (region I). From the discussion in the previous section, the pressure, temperature, and

Table 1 Analytical expressions for stability and control derivatives

Aerodynamic stability derivatives

$$(X_A)_{M_\infty} = -\gamma M_\infty P_\infty C_{p_N}\left[\sin^2\theta_L h + \sin^2(\alpha_0+\delta_0)\sin\delta_0\frac{S_{cs}}{b}\right]$$

$$(X_A)_\alpha = -q_\infty C_{p_N}\left[\sin(2\theta_L)h + \sin[2(\alpha_0+\delta_0)]\sin\delta_0\frac{S_{cs}}{b}\right]$$

$$(X_A)_q = q_\infty C_{p_N}\sin(2\theta_L)\frac{h}{V_\infty}\left[(h-\bar{z})\sin\alpha_0 - (L_1-\bar{x})\cos\alpha_0 + \tfrac{1}{2}l_1\cos\theta_L\right]$$

$$(X_A)_\eta = -\Delta\tau_1\left\{P_\infty L_1 + q_\infty C_{p_N}\left[\sin^2\theta_L L_1 + \sin(2\theta_L)h\right]\right\}$$

$$(X_A)_{\dot\eta} = \Delta\tau_1 q_\infty C_{p_N}\sin(2\theta_L)\frac{h}{V_\infty}\tfrac{1}{2}l_1\cos\theta_L$$

$$(Z_A)_{M_\infty} = -\gamma M_\infty P_\infty C_{p_N}\left[\sin^2\theta_L L_1 + \sin^2(\alpha_0+\delta_0)\cos\delta_0\frac{S_{cs}}{b}\right]$$

$$(Z_A)_\alpha = -q_\infty C_{p_N}\left[\sin(2\theta_L)L_1 + \sin[2(\alpha_0+\delta_0)]\cos\delta_0\frac{S_{cs}}{b}\right]$$

$$(Z_A)_q = q_\infty C_{p_N}\sin(2\theta_L)\frac{L_1}{V_\infty}\left[(h-\bar{z})\sin\alpha_0 - (L_1-\bar{x})\cos\alpha_0 + \tfrac{1}{2}l_1\cos\theta_L\right]$$

$$(Z_A)_\eta = \Delta\tau_1\left\{P_\infty h + q_\infty C_{p_N}\left[\sin^2\theta_L h - \sin(2\theta_L)L_1\right]\right\}$$

$$(Z_A)_{\dot\eta} = \Delta\tau_1 q_\infty C_{p_N}\sin(2\theta_L)\frac{L_1}{V_\infty}\tfrac{1}{2}l_1\cos\theta_L$$

$$(M_A)_{M_\infty} = P_\infty\gamma M_\infty C_{p_N}\left\{\sin^2\theta_L\left[\tfrac{1}{2}l_1^2 - (L_1-\bar{x})L_1 - (h-\bar{z})h\right] + \sin^2(\alpha_0+\delta_0)[x_{cs}\cos\delta_0 - z_{cs}\sin\delta_0]\frac{S_{cs}}{b}\right\}$$

$$(M_A)_\alpha = q_\infty C_{p_N}\left\{\sin(2\theta_L)\left[\tfrac{1}{2}l_1^2 - (L_1-\bar{x})L_1 - (h-\bar{z})h\right] + \sin[2(\alpha_0+\delta_0)][x_{cs}\cos\delta_0 - z_{cs}\sin\delta_0]\frac{S_{cs}}{b}\right\}$$

$$(M_A)_q = -\tfrac{1}{2}q_\infty C_{p_N}\sin(2\theta_L)\left\{\frac{l_1^2}{V_\infty}\left[\tfrac{2}{3}l_1\cos\theta_L - (L_1-\bar{x})\cos\alpha_0 + (h-\bar{z})\sin\alpha_0\right]\right.$$
$$\left. - \frac{z}{V_\infty}[L_1(L_1-\bar{x}) + h(h-\bar{z})]\left[\tfrac{1}{2}l_1\cos\theta_L - (L-\bar{x})\cos\alpha_0 + (h-\bar{z})\sin\alpha_0\right]\right\}$$

$$(M_A)_\eta = \Delta\tau_1\left\{\left[P_\infty + q_\infty C_{p_N}\sin^2\theta_L\right][(L_1-\bar{x})h - (h-\bar{z})L_1] + q_\infty C_{p_N}\sin(2\theta_L)\left[\tfrac{1}{2}l_1^2 - (L_1-\bar{x})L_1 - (h-\bar{z})h\right]\right\}$$

$$(M_A)_{\dot\eta} = -\Delta\tau_1 q_\infty C_{p_N}\sin(2\theta_L)\frac{l_1\cos\theta_L}{2V_\infty}\left[\tfrac{2}{3}l_1^2 - (L_1-\bar{x})L_1 - (h-\bar{z})h\right]$$

$$(Q_A)_{M_\infty} = \Delta\tau_1 P_\infty\gamma M_\infty C_{p_N}\sin^2\theta_L\tfrac{1}{2}l_1^2$$

$$(Q_A)_\alpha = \Delta\tau_1 q_\infty C_{p_N}\sin(2\theta_L)\tfrac{1}{2}l_1^2$$

$$(Q_A)_q = -\Delta\tau_1\tfrac{1}{2}q_\infty C_{p_N}\sin(2\theta_L)\frac{l_1^2}{V_\infty}\left[\tfrac{2}{3}l_1\cos\theta_L - (L_1-\bar{x})\cos\alpha_0 + (h-\bar{z})\sin\alpha_0\right]$$

$$(Q_A)_\eta = \Delta\tau_1^2 q_\infty C_{p_N}\sin(2\theta_L)\tfrac{1}{2}l_1^2$$

$$(Q_A)_{\dot\eta} = -\Delta\tau_1^2 q_\infty C_{p_N}\sin(2\theta_L)\frac{l_1\cos\theta_L}{V_\infty}\tfrac{1}{3}l_1^2$$

Aerodynamic control derivatives

$$(X_A)_\delta = -q_\infty C_{p_N}\left[\sin[2(\alpha_0+\delta_0)]\sin\delta_0 + \sin^2(\alpha_0+\delta_0)\cos\delta_0\right]\frac{S_{cs}}{b}$$

$$(Z_A)_\delta = -q_\infty C_{p_N}\left[\sin[2(\alpha_0+\delta_0)]\cos\delta_0 - \sin^2(\alpha_0+\delta_0)\sin\delta_0\right]\frac{S_{cs}}{b}$$

$$(M_A)_\delta = (X_A)_\delta z_{cs} - (Z_A)_\delta x_{cs}$$

$$(Q_A)_\delta = 0$$

Mach number along the vehicle's lower fore-body can be expressed in terms of the local flow deflection angle $\theta_L(s_1)$. If the location of the engine corresponds to $s_1 = 0$ (c.f. Fig. 2), then the pressure, temperature, and Mach number at the inlet to the engine are given by Eqs. (7–9) evaluated at $s_1 = 0$. It should be noted here that the interaction between the elastic airframe's aerodynamics and the propulsion system first becomes evident.

The expressions relating exit conditions to inlet conditions for each of the engine's three sections are given by the following.

For the diffuser,

$$\frac{\left[1+\tfrac{1}{2}(\gamma-1)M_2^2\right]^{(\gamma+1)/(\gamma-1)}}{M_2^2} = (\tilde{A}_D)^2\frac{\left[1+\tfrac{1}{2}(\gamma-1)M_1^2\right]^{(\gamma+1)/(\gamma-1)}}{M_1^2} \tag{17}$$

$$P_2 = P_1\left[\frac{1+\tfrac{1}{2}(\gamma-1)M_1^2}{1+\tfrac{1}{2}(\gamma-1)M_2^2}\right]^{\gamma/(\gamma-1)} \tag{18}$$

$$T_2 = T_1\frac{1+\tfrac{1}{2}(\gamma-1)M_1^2}{1+\tfrac{1}{2}(\gamma-1)M_2^2} \tag{19}$$

where M_2, P_2, and T_2 are the diffuser exit/combustor inlet (static) conditions and $\tilde{A}_D$ is the diffuser ratio defined as the ratio of the diffuser exit area to diffuser inlet area.

For the combustor,

$$\frac{M_3^2\left[1+\tfrac{1}{2}(\gamma-1)M_3^2\right]}{\left(\gamma M_3^2+1\right)^2} = \frac{M_2^2\left(1+\tfrac{1}{2}(\gamma-1)M_2^2\right)}{(\gamma M_2^2+1)^2} + \frac{M_2^2}{\left(\gamma M_2^2+1\right)^2}\frac{T_0}{T_2} \tag{20}$$

$$P_3 = P_2 \frac{1+\gamma M_2^2}{1+\gamma M_3^2} \tag{21}$$

$$T_3 = T_2 \left(\frac{1+\gamma M_2^2}{1+\gamma M_3^2} \frac{M_3}{M_2} \right)^2 \tag{22}$$

where M_3, P_3, and T_3 are the combustor exit/internal nozzle inlet (static) conditions and T_0 is the increase in total temperature across the combustor due to combustion of the fuel.

For the internal nozzle,

$$\frac{\left[1+\frac{1}{2}(\gamma-1)M_e^2\right]^{(\gamma+1)/(\gamma-1)}}{M_e^2} = (\bar{A}_N)^2 \frac{\left[1+\frac{1}{2}(\gamma-1)M_3^2\right]^{(\gamma+1)/(\gamma-1)}}{M_3^2} \tag{23}$$

$$P_e = P_3 \left[\frac{1+\frac{1}{2}(\gamma-1)M_3^2}{1+\frac{1}{2}(\gamma-1)M_e^2} \right]^{\gamma/(\gamma-1)} \tag{24}$$

$$T_e = T_3 \frac{1+\frac{1}{2}(\gamma-1)M_3^2}{1+\frac{1}{2}(\gamma-1)M_e^2} \tag{25}$$

where M_e, P_e, and T_e are the internal nozzle/engine exit (static) conditions and $\bar{A}_N$ is the internal nozzle ratio defined as the ratio of the nozzle exit area to nozzle inlet area.

Perturbations in engine exit conditions can now be related to perturbations in engine inlet conditions and engine control inputs through the use of engine sensitivity coefficients. The engine sensitivity coefficients are expressed in terms of the sensitivity coefficients for each of the engine's three sections.

Let the diffuser sensitivities be defined in the form

$$\begin{Bmatrix} \Delta M_2 \\ \Delta P_2 \\ \Delta T_2 \end{Bmatrix} = [D] \begin{Bmatrix} \Delta M_1 \\ \Delta P_1 \\ \Delta T_1 \end{Bmatrix} + [D_c]\{\Delta \bar{A}_D\} \tag{26}$$

where

$$[D] = \begin{bmatrix} \frac{\partial M_2}{\partial M_1} & \frac{\partial M_2}{\partial P_1} & \frac{\partial M_2}{\partial T_1} \\ \frac{\partial P_2}{\partial M_1} & \frac{\partial P_2}{\partial P_1} & \frac{\partial P_2}{\partial T_1} \\ \frac{\partial T_2}{\partial M_1} & \frac{\partial T_2}{\partial P_1} & \frac{\partial T_2}{\partial T_1} \end{bmatrix} \tag{27}$$

$$[D_c] = \begin{bmatrix} \frac{\partial M_2}{\partial \bar{A}_D} \\ \frac{\partial P_2}{\partial \bar{A}_D} \\ \frac{\partial T_2}{\partial \bar{A}_D} \end{bmatrix} \tag{28}$$

With the use of Eqs. (17–19), the diffuser sensitivities can be calculated and are listed in Table 2.

The combustor sensitivity coefficients are defined as follows:

$$\begin{Bmatrix} \Delta M_3 \\ \Delta P_3 \\ \Delta T_3 \end{Bmatrix} = [B] \begin{Bmatrix} \Delta M_2 \\ \Delta P_2 \\ \Delta T_2 \end{Bmatrix} + [B_c]\{\Delta T_0\} \tag{29}$$

where

$$[B] = \begin{bmatrix} \frac{\partial M_3}{\partial M_2} & \frac{\partial M_3}{\partial P_2} & \frac{\partial M_3}{\partial T_2} \\ \frac{\partial P_3}{\partial M_2} & \frac{\partial P_3}{\partial P_2} & \frac{\partial P_3}{\partial T_2} \\ \frac{\partial T_3}{\partial M_2} & \frac{\partial T_3}{\partial P_2} & \frac{\partial T_3}{\partial T_2} \end{bmatrix} \tag{30}$$

$$[B_c] = \begin{bmatrix} \frac{\partial M_3}{\partial T_0} \\ \frac{\partial P_3}{\partial T_0} \\ \frac{\partial T_3}{\partial T_0} \end{bmatrix} \tag{31}$$

With the use of Eqs. (20–22), the combustor sensitivities can be calculated and are listed in Table 2.

The internal nozzle sensitivity coefficients are defined as follows:

$$\begin{Bmatrix} \Delta M_e \\ \Delta P_e \\ \Delta T_e \end{Bmatrix} = [N] \begin{Bmatrix} \Delta M_3 \\ \Delta P_3 \\ \Delta T_3 \end{Bmatrix} \tag{32}$$

where

$$[N] = \begin{bmatrix} \frac{\partial M_e}{\partial M_3} & \frac{\partial M_e}{\partial P_3} & \frac{\partial M_e}{\partial T_3} \\ \frac{\partial P_e}{\partial M_3} & \frac{\partial P_e}{\partial P_3} & \frac{\partial P_e}{\partial T_3} \\ \frac{\partial T_e}{\partial M_3} & \frac{\partial T_e}{\partial P_3} & \frac{\partial T_e}{\partial T_3} \end{bmatrix} \tag{33}$$

With the use of Eqs. (23–25), the internal nozzle sensitivities can be calculated and are listed in Table 2.

With the diffuser, combustor, and internal nozzle sensitivity coefficients known, the sensitivity coefficients for the entire engine module can now be obtained. Combining Eqs. (26), (29), and (32), the engine sensitivities are given by

$$\begin{Bmatrix} \Delta M_e \\ \Delta P_e \\ \Delta T_e \end{Bmatrix} = [\bar{E}] \begin{Bmatrix} \Delta M_1 \\ \Delta P_1 \\ \Delta T_1 \end{Bmatrix} + [\bar{E}_c] \begin{Bmatrix} \Delta \bar{A}_D \\ \Delta T_0 \end{Bmatrix} \tag{34}$$

where

$$[\bar{E}] = \begin{bmatrix} \frac{\partial M_e}{\partial M_1} & \frac{\partial M_e}{\partial P_1} & \frac{\partial M_e}{\partial T_1} \\ \frac{\partial P_e}{\partial M_1} & \frac{\partial P_e}{\partial P_1} & \frac{\partial P_e}{\partial T_1} \\ \frac{\partial T_e}{\partial M_1} & \frac{\partial T_e}{\partial P_1} & \frac{\partial T_e}{\partial T_1} \end{bmatrix} = [NBD] \tag{35}$$

$$[\bar{E}_c] = \begin{bmatrix} \frac{\partial M_e}{\partial \bar{A}_D} & \frac{\partial M_e}{\partial T_0} \\ \frac{\partial P_e}{\partial \bar{A}_D} & \frac{\partial P_e}{\partial T_0} \\ \frac{\partial T_e}{\partial \bar{A}_D} & \frac{\partial T_e}{\partial T_0} \end{bmatrix} = [NBD_c \quad NB_c] \tag{36}$$

The thrust per unit width of the engine module can be expressed as[9]

$$\mathrm{Th} = \left(\left[\gamma P_e M_e^2 + (P_e - P_\infty) \right] - \frac{\gamma P_1 M_1^2 + (P_1 - P_\infty)}{\bar{A}_D \bar{A}_N} \right) \frac{A_e}{b} \tag{37}$$

or

$$\mathrm{Th} = f_{\mathrm{Th}}(M_1, P_1, M_e, P_e, \bar{A}_D) \tag{38}$$

With the use of Eqs. (34) and (37), the perturbation in the engine module thrust due to perturbations in the engine inlet conditions and to the engine control inputs can be written in matrix form as

$$\Delta \mathrm{Th} = [F] \begin{Bmatrix} \Delta M_1 \\ \Delta P_1 \\ \Delta T_1 \end{Bmatrix} + [F_c] \begin{Bmatrix} \Delta \bar{A}_D \\ \Delta T_0 \end{Bmatrix} \tag{39}$$

Table 2 Engine sensitivities

Diffuser sensitivities

$$\frac{\partial M_2}{\partial M_1} = \frac{M_2\left[1+\frac{1}{2}(\gamma-1)M_2^2\right]\left(M_1^2-1\right)}{M_1\left[1+\frac{1}{2}(\gamma-1)M_1^2\right]\left(M_2^2-1\right)} \qquad \frac{\partial M_2}{\partial P_1} = 0 \qquad \frac{\partial M_2}{\partial T_1} = 0$$

$$\frac{\partial P_2}{\partial M_1} = P_2\left(\frac{\gamma M_1}{1+\frac{1}{2}(\gamma-1)M_1^2} - \frac{\gamma M_2}{1+\frac{1}{2}(\gamma-1)M_2^2}\frac{\partial M_2}{\partial M_1}\right) \qquad \frac{\partial P_2}{\partial P_1} = \frac{P_2}{P_1} \qquad \frac{\partial P_2}{\partial T_1} = 0$$

$$\frac{\partial T_2}{\partial M_1} = T_2\left(\frac{(\gamma-1)M_1}{1+\frac{1}{2}(\gamma-1)M_1^2} - \frac{(\gamma-1)M_2}{1+\frac{1}{2}(\gamma-1)M_2^2}\frac{\partial M_2}{\partial M_1}\right) \qquad \frac{\partial T_2}{\partial P_1} = 0 \qquad \frac{\partial T_2}{\partial T_1} = \frac{T_2}{T_1}$$

$$\frac{\partial M_2}{\partial \bar{A}_D} = \frac{M_2\left[1+\frac{1}{2}(\gamma-1)M_2^2\right]}{\bar{A}_D\left(M_2^2-1\right)} \qquad \frac{\partial P_2}{\partial \bar{A}_D} = -P_2\frac{\gamma M_2}{1+\frac{1}{2}(\gamma-1)M_2^2}\frac{\partial M_2}{\partial \bar{A}_D} \qquad \frac{\partial T_2}{\partial \bar{A}_D} = -T_2\frac{(\gamma-1)M_2}{1+\frac{1}{2}(\gamma-1)M_2^2}\frac{\partial M_2}{\partial \bar{A}_D}$$

Combustor sensitivities

$$\frac{\partial M_3}{\partial M_2} = \frac{M_2\left(\gamma M_3^2+1\right)^3\left[\left(M_2^2-1\right)+\left(\gamma M_2^2-1\right)(T_0/T_2)\right]}{M_3\left(\gamma M_2^2+1\right)^3\left(M_3^2-1\right)} \qquad \frac{\partial M_3}{\partial P_2} = 0$$

$$\frac{\partial M_3}{\partial T_2} = \frac{M_2^2}{2M_3}\frac{\left(\gamma M_3^2+1\right)^3}{\left(M_3^2-1\right)\left(\gamma M_2^2+1\right)^2}\frac{T_0}{T_2^2}$$

$$\frac{\partial P_3}{\partial M_2} = P_3\left(\frac{2\gamma M_2}{\gamma M_2^2+1} - \frac{2\gamma M_3}{\gamma M_3^2+1}\frac{\partial M_3}{\partial M_2}\right) \qquad \frac{\partial P_3}{\partial P_2} = \frac{P_3}{P_2}$$

$$\frac{\partial P_3}{\partial T_2} = -P_3\frac{2\gamma M_3}{\gamma M_3^2+1}\frac{\partial M_3}{\partial T_2}$$

$$\frac{\partial T_3}{\partial M_2} = T_3\left(\frac{2\left(\gamma M_2^2-1\right)}{M_2\left(\gamma M_2^2+1\right)} - \frac{2\left(\gamma M_3^2-1\right)}{M_3\left(\gamma M_3^2+1\right)}\frac{\partial M_3}{\partial M_2}\right) \qquad \frac{\partial T_3}{\partial P_2} = 0$$

$$\frac{\partial T_3}{\partial T_2} = \frac{T_3}{T_2} - T_3\frac{2\left(\gamma M_3^2-1\right)}{M_3\left(\gamma M_3^2+1\right)}\frac{\partial M_3}{\partial T_2}$$

$$\frac{\partial M_3}{\partial T_0} = -\frac{\partial M_3}{\partial T_2}\frac{T_2}{T_0} \qquad \frac{\partial P_3}{\partial T_0} = -P_3\frac{2\gamma M_3}{\gamma M_3^2+1}\frac{\partial M_3}{\partial T_0} \qquad \frac{\partial T_3}{\partial T_0} = -T_3\frac{2\left(\gamma M_3^2-1\right)}{M_3\left(\gamma M_3^2+1\right)}\frac{\partial M_3}{\partial T_0}$$

Internal nozzle sensitivities

$$\frac{\partial M_e}{\partial M_3} = \frac{M_e\left[\frac{1}{2}(\gamma-1)M_e^2\right]\left(M_3^2-1\right)}{M_3\left[1+\frac{1}{2}(\gamma-1)M_3^2\right]\left(M_e^2-1\right)} \qquad \frac{\partial M_e}{\partial P_3} = 0 \qquad \frac{\partial M_e}{\partial T_3} = 0$$

$$\frac{\partial P_e}{\partial M_3} = P_e\left(\frac{\gamma M_3}{1+\frac{1}{2}(\gamma-1)M_3^2} - \frac{\gamma M_e}{1+\frac{1}{2}(\gamma-1)M_e^2}\frac{\partial M_e}{\partial M_3}\right) \qquad \frac{\partial P_e}{\partial P_3} = \frac{P_e}{P_3} \qquad \frac{\partial P_e}{\partial T_3} = 0$$

$$\frac{\partial T_e}{\partial M_3} = T_e\left(\frac{(\gamma-1)M_3}{1+\frac{1}{2}(\gamma-1)M_3^2} - \frac{(\gamma-1)M_e}{1+\frac{1}{2}(\gamma-1)M_e^2}\frac{\partial M_e}{\partial M_3}\right) \qquad \frac{\partial T_e}{\partial P_3} = 0 \qquad \frac{\partial T_e}{\partial T_3} = \frac{T_e}{T_3}$$

where

$$[F] = \begin{bmatrix}\frac{\partial \mathrm{Th}}{\partial M_1} & \frac{\partial \mathrm{Th}}{\partial P_1} & \frac{\partial \mathrm{Th}}{\partial T_1}\end{bmatrix} = [T_1 + T_e\bar{E}] \tag{40}$$

$$[F_c] = \begin{bmatrix}\frac{\partial \mathrm{Th}}{\partial \bar{A}_D} & \frac{\partial \mathrm{Th}}{\partial T_0}\end{bmatrix} = [T_c + T_e\bar{E}_c] \tag{41}$$

and

$$[T_1] = \begin{bmatrix}\frac{\partial f_{\mathrm{Th}}}{\partial M_1} & \frac{\partial f_{\mathrm{Th}}}{\partial P_1} & \frac{\partial f_{\mathrm{Th}}}{\partial T_1}\end{bmatrix} \tag{42}$$

$$\frac{\partial f_{\mathrm{Th}}}{\partial M_1} = -2\gamma\frac{P_1M_1}{\bar{A}_D\bar{A}_N}\frac{A_e}{b} \tag{42a}$$

$$\frac{\partial f_{\mathrm{Th}}}{\partial P_1} = -\frac{\left(\gamma M_1^2+1\right)}{\bar{A}_D\bar{A}_N}\frac{A_e}{b} \tag{42b}$$

$$\frac{\partial f_{\mathrm{Th}}}{\partial T_1} = 0 \tag{42c}$$

$$[T_e] = \begin{bmatrix}\frac{\partial f_{\mathrm{Th}}}{\partial M_e} & \frac{\partial f_{\mathrm{Th}}}{\partial P_e} & \frac{\partial f_{\mathrm{Th}}}{\partial T_e}\end{bmatrix} \tag{43}$$

$$\frac{\partial f_{\mathrm{Th}}}{\partial M_e} = 2\gamma P_eM_e\frac{A_e}{b} \tag{43a}$$

$$\frac{\partial f_{\mathrm{Th}}}{\partial P_e} = \left(\gamma M_e^2+1\right)\frac{A_e}{b} \tag{43b}$$

$$\frac{\partial f_{\mathrm{Th}}}{\partial T_e} = 0 \tag{43c}$$

$$[T_c] = \begin{bmatrix}\frac{\partial f_{\mathrm{Th}}}{\partial \bar{A}_D} & \frac{\partial f_{\mathrm{Th}}}{\partial T_0}\end{bmatrix} \tag{44}$$

$$\frac{\partial f_{\mathrm{Th}}}{\partial \bar{A}_D} = \left[\gamma P_1M_1^2 + (P_1 - P_\infty)\right]\frac{1}{\bar{A}_D^2\bar{A}_N}\frac{A_e}{b} \tag{44a}$$

$$\frac{\partial f_{\mathrm{Th}}}{\partial T_0} = 0 \tag{44b}$$

Using Eq. (40), the thrust sensitivity coefficients relating the perturbation in engine module thrust to the perturbations in the aerodynamic parameters of region I are given by

$$\frac{\partial \mathrm{Th}}{\partial M_\infty} = \frac{\partial \mathrm{Th}}{\partial M_1}\frac{\partial M_1}{\partial M_\infty} + \frac{\partial \mathrm{Th}}{\partial P_1}\frac{\partial P_1}{\partial M_\infty} + \frac{\partial \mathrm{Th}}{\partial T_1}\frac{\partial T_1}{\partial M_\infty} \tag{45}$$

$$\frac{\partial \mathrm{Th}}{\partial \theta_L} = \frac{\partial \mathrm{Th}}{\partial M_1}\frac{\partial M_1}{\partial \theta_L} + \frac{\partial \mathrm{Th}}{\partial P_1}\frac{\partial P_1}{\partial \theta_L} + \frac{\partial \mathrm{Th}}{\partial T_1}\frac{\partial T_1}{\partial \theta_L} \tag{46}$$

where from Eqs. (7–9),

$$\frac{\partial M_1}{\partial M_\infty} = \frac{\cos\theta_L}{\left[1 + \frac{1}{2}(\gamma - 1)M_\infty^2 \sin^2\theta_L\right]^{3/2}} \tag{47a}$$

$$\frac{\partial M_1}{\partial \theta_L} = -\frac{M_\infty\left[1 + \frac{1}{2}(\gamma - 1)M_\infty^2\right]\sin\theta_L}{\left[1 + \frac{1}{2}(\gamma - 1)M_\infty^2 \sin^2\theta_L\right]^{3/2}} \tag{47b}$$

$$\frac{\partial P_1}{\partial M_\infty} = P_\infty \gamma M_\infty C_{p_N} \sin^2\theta_L \tag{48a}$$

$$\frac{\partial P_1}{\partial \theta_L} = P_\infty \tfrac{1}{2}\gamma M_\infty^2 C_{p_N} \sin(2\theta_L) \tag{48b}$$

$$\frac{\partial T_1}{\partial M_\infty} = T_\infty(\gamma - 1)M_\infty \sin^2\theta_L \tag{49a}$$

$$\frac{\partial T_1}{\partial \theta_L} = T_\infty \tfrac{1}{2}(\gamma - 1)M_\infty^2 \sin(2\theta_L) \tag{49b}$$

and the thrust sensitivity coefficients relating the perturbation in engine thrust to the engine control inputs are given by Eq. (41).

Now, let the set of linearized equations for the perturbation thrust forces and moment, expressed in terms of the thrust stability derivatives and the thrust control derivatives, be given in matrix form as

$$\begin{Bmatrix} \Delta X_T \\ \Delta Z_T \\ \Delta M_T \\ \Delta Q_T \end{Bmatrix} = [T]\begin{Bmatrix} \Delta M_\infty \\ \Delta\alpha \\ \Delta q \\ \Delta\eta \\ \Delta\dot{\eta} \end{Bmatrix} + [T_c]\begin{Bmatrix} \Delta \bar{A}_D \\ \Delta T_0 \end{Bmatrix} \tag{50}$$

where

$$[T] = \begin{bmatrix} (X_T)_{M_\infty} & (X_T)_\alpha & (X_T)_q & (X_T)_\eta & (X_T)_{\dot{\eta}} \\ 0 & 0 & 0 & 0 & 0 \\ (M_T)_{M_\infty} & (M_T)_\alpha & (M_T)_q & (M_T)_\eta & (M_T)_{\dot{\eta}} \\ 0 & 0 & 0 & 0 & 0 \end{bmatrix} \tag{51}$$

$$[T_c] = \begin{bmatrix} (X_T)_{\bar{A}_D} & (X_T)_{T_0} \\ 0 & 0 \\ (M_T)_{\bar{A}_D} & (M_T)_{T_0} \\ 0 & 0 \end{bmatrix} \tag{52}$$

where the subscript in the above matrices refers to the partial derivative with respect to that quantity.

The engine-thrust stability and control derivatives can be obtained in terms of the thrust sensitivity coefficients,[9] i.e., Eqs. (41–46), and are listed in Table 3.

External Nozzle Analysis

From Fig. 2, the flow of the engine's exhaust gas is bounded from above by the vehicle's afterbody/nozzle surface and from below by a shear layer between the exhaust gas and the freestream atmosphere (region II). These boundaries define the external nozzle.

It is evident, then, that the pressure distribution over the vehicle's afterbody/nozzle surface is dependent on the shape of the external nozzle, which is in turn dependent on both the flow in region I and the exit conditions from the engine. Here again there is strong interaction between the elastic airframe's aerodynamics and the propulsion system.

Along the shear layer, the pressure differential across the shear must be zero. By matching the inner pressure, calculated from quasi-one-dimensional, isentropic flow, with the outer pressure, calculated from Newtonian impact theory, the position of the shear layer may be determined. With the position of the shear layer known, the pressure distribution along the afterbody/nozzle surface can be determined. As shown in Ref. 9, the pressure distribution along the afterbody/nozzle surface can be approximated as

$$P_2(s_2) \approx \frac{P_e}{1 + (s_2/l_2)(P_e/P_\infty - 1)} \tag{53}$$

where P_e is the pressure at the engine exit, P_∞ is the freestream pressure, l_2 is the length of the vehicle's afterbody/nozzle surface, and s_2 is the distance from the vehicle's lower apex to the point of interest along the vehicle's afterbody/nozzle surface (cf. Fig. 2).

It should be noted here that, in using Eq. (53), it is assumed that the exhaust gas is ideally expanded and that any perturbations in the freestream Mach number and angle of attack do not produce a change in the position of the shear layer; i.e., the "shape" of the external nozzle does not change with respect to the vehicle's x and y axes. Any perturbation in the external nozzle pressure distribution is due only to perturbations in the engine exit pressure P_e and the elastic motion of the afterbody/nozzle surface.

As a first approximation, Eq. (53) is used to estimate the following stability derivatives. The forces and moment due to the flow in the

Table 3 Stability and control derivatives due to engine-module thrust

Engine-thrust stability derivatives

$$(X_T)_{M_\infty} = \frac{\partial \mathrm{Th}}{\partial M_\infty} \qquad (X_T)_\alpha = \frac{\partial \mathrm{Th}}{\partial \theta_L}$$

$$(X_T)_q = -\frac{1}{V_\infty}\left[(h - \bar{z})\sin\alpha_0 - (L_1 - \bar{x})\cos\alpha_0\right]\frac{\partial \mathrm{Th}}{\partial \theta_L}$$

$$(X_T)_\eta = \Delta\tau_1 \frac{\partial \mathrm{Th}}{\partial \theta_L} \qquad (X_T)_{\dot{\eta}} = 0$$

$$(M_T)_{M_\infty} = (h - \bar{z})\frac{\partial \mathrm{Th}}{\partial M_\infty} \qquad (M_T)_\alpha = (h - \bar{z})\frac{\partial \mathrm{Th}}{\partial \theta_L}$$

$$(M_T)_q = -\frac{1}{V_\infty}[(h - \bar{z})\sin\alpha_0 - (L_1 - \bar{x})\cos\alpha_0](h - \bar{z})\frac{\partial \mathrm{Th}}{\partial \theta_L}$$

$$(M_T)_\eta = \Delta\tau_1(h - \bar{z})\frac{\partial \mathrm{Th}}{\partial \theta_L} \qquad (M_T)_{\dot{\eta}} = 0$$

Engine-thrust control derivatives

$$(X_T)_{\bar{A}_D} = \frac{\partial \mathrm{Th}}{\partial \bar{A}_D} \qquad (X_T)_{T_0} = \frac{\partial \mathrm{Th}}{\partial T_o} \qquad (M_T)_{\bar{A}_D} = (h - \bar{z})\frac{\partial \mathrm{Th}}{\partial \bar{A}_D} \qquad (M_T)_{T_o} = (h - \bar{z})\frac{\partial \mathrm{Th}}{\partial T_0}$$

Table 4 Stability and control derivatives due to external nozzle

External nozzle stability derivatives

$$(X_E)_{M_\infty} = hI_1\frac{\partial P_e}{\partial M_\infty} \qquad (X_E)_\alpha = hI_1\frac{\partial P_e}{\partial \theta_L} \qquad (X_E)_q = -\frac{h}{V_\infty}[(h-\bar{z})\sin\alpha_0 - (L_1-\bar{x})\cos\alpha_0]I_1\frac{\partial P_e}{\partial \theta_L}$$

$$(X_E)_\eta = \Delta\tau_1 hI_1\frac{\partial P_e}{\partial \theta_L} + \Delta\tau_2 L_2 P_\infty\frac{\bar{P}\ln(\bar{P})}{\bar{P}-1} \qquad (X_E)_{\dot\eta} = 0$$

$$(Z_E)_{M_\infty} = -L_2 I_1\frac{\partial P_e}{\partial M_\infty} \qquad (Z_E)_\alpha = -L_2 I_1\frac{\partial P_e}{\partial \theta_L} \qquad (Z_E)_q = \frac{L_2}{V_\infty}\Big[(h-\bar{z})\sin\alpha_0 - (L_1-\bar{x})\cos\alpha_0\Big]I_1\frac{\partial P_e}{\partial \theta_L}$$

$$(Z_E)_\eta = -\Delta\tau_1 L_2 I_1\frac{\partial P_e}{\partial \theta_L} + \Delta\tau_2 hP_\infty\frac{\bar{P}\ln(\bar{P})}{\bar{P}-1} \qquad (Z_E)_{\dot\eta} = 0$$

$$(M_E)_{M_\infty} = \Big\{[(h-\bar{z})h - (L_1-\bar{x})L_2]I_1 - l_2^2 I_2\Big\}\frac{\partial P_e}{\partial M_\infty} \qquad (M_E)_\alpha = \Big\{[(h-\bar{z})h - (L_1-\bar{x})L_2]I_1 - l_2^2 I_2\Big\}\frac{\partial P_e}{\partial \theta_L}$$

$$(M_E)_q = -\frac{1}{V_\infty}\Big[(h-\bar{z})\sin\alpha_0 - (L_1-\bar{x})\cos\alpha_0\Big]\Big\{[(h-\bar{z})h - (L_1-\bar{x})L_2]I_1 - l_2^2 I_2\Big\}\frac{\partial P_e}{\partial \theta_L}$$

$$(M_E)_\eta = \Delta\tau_1\Big\{[(h-\bar{z})h - (L_1-\bar{x})L_2]I_1 - l_2^2 I_2\Big\}\frac{\partial P_e}{\partial \theta_L} + \Delta\tau_2[(h-\bar{z})L_2 + (L_1-\bar{x})h]P_\infty\frac{\bar{P}\ln(\bar{P})}{\bar{P}-1}$$

$$(M_E)_{\dot\eta} = 0$$

$$(Q_E)_{M_\infty} = \Delta\tau_2\, l_2^2 I_2\frac{\partial P_e}{\partial M_\infty} \qquad (Q_E)_\alpha = \Delta\tau_2\, l_2^2 I_2\frac{\partial P_e}{\partial \theta_L} \qquad (Q_E)_q = -\Delta\tau_2\frac{l_2^2}{V_\infty}[(h-\bar{z})\sin\alpha_0 - (L_1-\bar{x})\cos\alpha_0]I_2\frac{\partial P_e}{\partial \theta_L}$$

$$(Q_E)_\eta = \Delta\tau_1\Delta\tau_2\, l_2^2 I_2\frac{\partial P_e}{\partial \theta_L} \qquad (Q_E)_{\dot\eta} = 0$$

External nozzle control derivatives

$$(X_E)_{\bar{A}_D} = hI_1\frac{\partial P_e}{\partial \bar{A}_D} \qquad (X_E)_{T_0} = hI_1\frac{\partial P_e}{\partial T_0}$$

$$(Z_E)_{\bar{A}_D} = -L_2 I_1\frac{\partial P_e}{\partial \bar{A}_D} \qquad (Z_E)_{T_0} = -L_2 I_1\frac{\partial P_e}{\partial T_0}$$

$$(M_E)_{\bar{A}_D} = \Big\{[(h-\bar{z})h - (L_1-\bar{x})L_2]I_1 - l_2^2 I_2\Big\}\frac{\partial P_e}{\partial \bar{A}_D} \qquad (M_E)_{T_0} = \Big\{[(h-\bar{z})h - (L_1-\bar{x})L_2]I_1 - l_2^2 I_2\Big\}\frac{\partial P_e}{\partial T_0}$$

$$(Q_E)_{\bar{A}_D} = \Delta\tau_2\, l_2^2 I_2\frac{\partial P_e}{\partial \bar{A}_D} \qquad (Q_E)_{T_0} = \Delta\tau_2\, l_2^2 I_2\frac{\partial P_e}{\partial T_0}$$

external nozzle can be expressed as[9]

$$X_E = P_\infty l_2\frac{\bar{P}\ln(\bar{P})}{\bar{P}-1}\sin(\tau_2 + \Delta\tau_2\eta) \tag{54}$$

$$Z_E = -P_\infty l_2\frac{\bar{P}\ln(\bar{P})}{\bar{P}-1}\cos(\tau_2 + \Delta\tau_2\eta) \tag{55}$$

$$M_E = P_\infty\left[l_2 r_2\frac{\bar{P}\ln(\bar{P})}{\bar{P}-1} - l_2^2\frac{\bar{P}}{\bar{P}-1}\left(1 - \frac{\ln(\bar{P})}{\bar{P}-1}\right)\right] \tag{56}$$

$$Q_E = \Delta\tau_2 P_\infty l_2^2\frac{\bar{P}}{\bar{P}-1}\left[1 - \frac{\ln(\bar{P})}{\bar{P}-1}\right] \tag{57}$$

where

$$\bar{P} = \frac{P_e}{P_\infty}, \qquad r_2 = (h-\bar{z})\sin(\tau_t) - (L_1-\bar{x})\cos(\tau_t)$$

Given the above expressions, the stability derivatives due to the exhaust flow in the external nozzle can be evaluated.

Let the linearized equations for the perturbation external nozzle forces and moment, written in terms of the external nozzle stability derivatives and the external nozzle control derivatives, be given in matrix form as

$$\begin{Bmatrix}\Delta X_E\\ \Delta Z_E\\ \Delta M_E\\ \Delta Q_E\end{Bmatrix} = [E]\begin{Bmatrix}\Delta M_\infty\\ \Delta\alpha\\ \Delta q\\ \Delta\eta\\ \Delta\dot\eta\end{Bmatrix} + [E_c]\begin{Bmatrix}\Delta\bar{A}_D\\ \Delta T_0\end{Bmatrix} \tag{58}$$

where

$$[E] = \begin{bmatrix}(X_E)_{M_\infty} & (X_E)_\alpha & (X_E)_q & (X_E)_\eta & (X_E)_{\dot\eta}\\ (Z_E)_{M_\infty} & (Z_E)_\alpha & (Z_E)_q & (Z_E)_\eta & (Z_E)_{\dot\eta}\\ (M_E)_{M_\infty} & (M_E)_\alpha & (M_E)_q & (M_E)_\eta & (M_E)_{\dot\eta}\\ (Q_E)_{M_\infty} & (Q_E)_\alpha & (Q_E)_q & (Q_E)_\eta & (Q_E)_{\dot\eta}\end{bmatrix} \tag{59}$$

$$[E_C] = \begin{bmatrix}(X_E)_{\bar{A}_D} & (X_E)_{T_0}\\ (Z_E)_{\bar{A}_D} & (Z_E)_{T_0}\\ (M_E)_{\bar{A}_D} & (M_E)_{T_0}\\ (Q_E)_{\bar{A}_D} & (Q_E)_{T_0}\end{bmatrix} \tag{60}$$

where the subscripts in the above matrices refer to the partial derivative with respect to that quantity. The stability and control derivatives can be expressed in terms of the exit pressure sensitivity coefficients. With the use of Eq. (35), which relates the perturbation in exit pressure to the perturbations at the engine inlet, and Eqs. (47–49), one can determine the exit pressure sensitivity coefficients that relate perturbations in exit pressure to perturbations in the aerodynamic parameters of region I, or

$$\frac{\partial P_e}{\partial M_\infty} = \frac{\partial P_e}{\partial M_1}\frac{\partial M_1}{\partial M_\infty} + \frac{\partial P_e}{\partial P_1}\frac{\partial P_1}{\partial M_\infty} + \frac{\partial P_e}{\partial T_1}\frac{\partial T_1}{\partial M_\infty} \tag{61}$$

$$\frac{\partial P_e}{\partial \theta_L} = \frac{\partial P_e}{\partial M_1}\frac{\partial M_1}{\partial \theta_L} + \frac{\partial P_e}{\partial P_1}\frac{\partial P_1}{\partial \theta_L} + \frac{\partial P_e}{\partial T_1}\frac{\partial T_1}{\partial \theta_L} \tag{62}$$

The exit pressure sensitivity coefficients that relate perturbations in the exit pressure to the engine control terms are given by Eq. (36). Finally, the external nozzle stability derivatives and the external nozzle control derivatives are listed in Table 4.

Vehicle Dynamics

The longitudinal equations of motion to be considered here are

$$\dot{h} = V\sin(\theta - \alpha) \tag{63}$$

$$m(\dot{u} + wq) = X - mg\sin(\theta) \tag{64}$$

$$m(\dot{w} - uq) = Z + mg\cos(\theta) \tag{65}$$

$$I_{yy}\dot{q} = M \tag{66}$$

Equations (63–66), linearized with respect to an equilibrium flight condition, yield the linearized perturbation equations

$$\Delta\dot{h} = -u_0\Delta\alpha + u_0\Delta\theta \tag{67}$$

$$\Delta\dot{u} = -g\Delta\theta + \frac{\Delta X}{m} \tag{68}$$

$$\Delta\dot{\alpha} = \frac{\Delta\dot{w}}{u_0} = \Delta q + \frac{\Delta Z}{u_0 m} \tag{69}$$

$$\Delta\dot{\theta} = \Delta q \tag{70}$$

$$\Delta\dot{q} = \frac{\Delta M}{I_{yy}} \tag{71}$$

where $u_0 = M_\infty a_\infty$, g is the acceleration due to gravity, and the delta quantities are the perturbations from the equilibrium flight condition.

With undamped natural frequency ω_1 and damping ratio ζ_1 the perturbed equation of motion describing the elastic degree of freedom is governed by

$$\Delta\ddot{\eta} = -\omega_1^2\Delta\eta - 2\zeta_1\omega_1\Delta\dot{\eta} + \frac{\Delta Q}{\mathrm{m}} \tag{72}$$

Defining the state vector $\boldsymbol{x}$, the force vector $\boldsymbol{F}$, and the control vector $\boldsymbol{u}$ as

$$\boldsymbol{x} = \begin{pmatrix} \Delta h\ (\mathrm{ft}) \\ \Delta u\ (\mathrm{ft/s}) \\ \Delta\alpha\ (\mathrm{rad}) \\ \Delta\theta\ (\mathrm{rad}) \\ \Delta q\ (\mathrm{rad/s}) \\ \Delta\tau_1\eta\ (\mathrm{rad}) \\ \Delta\tau_1\dot{\eta}\ (\mathrm{rad/s}) \end{pmatrix}, \qquad \boldsymbol{F} = \begin{pmatrix} \Delta X\ (\mathrm{lb/ft}) \\ \Delta Z\ (\mathrm{lb/ft}) \\ \Delta M\ (\mathrm{ft\cdot lb/ft}) \\ \Delta Q\ (\mathrm{ft\cdot lb/ft}) \end{pmatrix},$$

$$\boldsymbol{u} = \begin{pmatrix} \Delta\delta\ (\mathrm{rad}) \\ \Delta\bar{A}_D \\ \Delta T_0\ (\mathrm{deg\ R}) \end{pmatrix}$$

Equations (67–72) can be expressed in state-space form as follows.

With the state vector and force vector defined above, Eqs. (67–72) can be expressed as

$$\dot{\boldsymbol{x}} = [T_1]\boldsymbol{x} + [T_2]\boldsymbol{F} \tag{73}$$

where the matrices $[T_1]$ and $[T_2]$ are defined as

$$[T_1] = \begin{bmatrix} 0 & 0 & -u_0 & u_0 & 0 & 0 & 0 \\ 0 & 0 & -g & 0 & 0 & 0 & 0 \\ 0 & 0 & 0 & 0 & 1 & 0 & 0 \\ 0 & 0 & 0 & 0 & 1 & 0 & 0 \\ 0 & 0 & 0 & 0 & 0 & 0 & 0 \\ 0 & 0 & 0 & 0 & 0 & 0 & 1 \\ 0 & 0 & 0 & 0 & 0 & -\omega_1^2 & -2\zeta_1\omega_1 \end{bmatrix}$$

$$[T_2] = \begin{bmatrix} 0 & 0 & 0 & 0 \\ 1/m & 0 & 0 & 0 \\ 0 & 1/mu_0 & 0 & 0 \\ 0 & 0 & 0 & \\ 0 & 0 & 1/I_{yy} & 0 \\ 0 & 0 & 0 & 0 \\ 0 & 0 & 0 & \Delta\tau_1/\mathrm{m} \end{bmatrix}$$

(Note, here, that for a two-dimensional analysis of the vehicle, all masses, inertia, forces, and moments are normalized per unit vehicle width.) With the use of Eqs. (15), (16), (51), (52), (59), and (60), the integrated stability-and-control derivative matrices can be expressed as

$$[S] = [A + T + E] \tag{74}$$

$$[S_c] = \left[A_c \vdots (T_c + E_c)\right] \tag{75}$$

which gives, for the force vector,

$$\boldsymbol{F} = \left[\begin{array}{c} c_1S_{11} \\ c_1S_{21} \\ \hdashline c_1S_{31} \\ c_1S_{41} \end{array}\right] [T_3]\boldsymbol{x} + [S_c]\boldsymbol{u} \tag{76}$$

where the transformation matrix $[T_3]$ is given as

$$[T_3] = \begin{bmatrix} 1 & 0 & 0 & 0 & 0 & 0 & 0 \\ 0 & 1/a_\infty & 0 & 0 & 0 & 0 & 0 \\ 0 & 0 & 1 & 0 & 0 & 0 & 0 \\ 0 & 0 & 0 & 0 & 1 & 0 & 0 \\ 0 & 0 & 0 & 0 & 0 & 1/\Delta\tau_1 & 0 \\ 0 & 0 & 0 & 0 & 0 & 0 & 1/\Delta\tau_1 \end{bmatrix}$$

Here, the stability derivatives due to altitude perturbations, Δh, are estimated through the relationship

$$\frac{\partial(\cdot)}{\partial h} = c_1\frac{\partial(\cdot)}{\partial M_\infty} \tag{77}$$

with c_1 given by

$$c_1 = \frac{(\partial q_\infty/\partial P_\infty)(\mathrm{d}P_\infty/\mathrm{d}h)}{\partial q_\infty/\partial M_\infty} = \frac{M_\infty}{2P_\infty}\frac{\mathrm{d}P_\infty}{\mathrm{d}h} \tag{78}$$

Substituting Eq. (76) for $\boldsymbol{F}$, Eq. (73) can be written as

$$\dot{\boldsymbol{x}} = [A_{ss}]\boldsymbol{x} + [B_{ss}]\boldsymbol{u} \tag{79}$$

with

$$[A_{ss}] = [T_1] + [T_2]\left[\begin{array}{c} c_1S_{11} \\ c_1S_{21} \\ \hdashline c_1S_{31} \\ c_1S_{41} \end{array}\right] [T_3] \tag{80}$$

$$[B_{ss}] = [T_2][S_c] \tag{81}$$

With the system matrix known from Eq. (80), a modal analysis can be performed to investigate the dynamic characteristics of the generic elastic study-vehicle configuration.

Numerical Results

Consider a vehicle configuration and nominal flight condition as given below.

The vehicle geometry is given by

$\tau_1 = 14.00$ deg,	$\tau_2 = 20.00$ deg
$L = 150.00$ ft,	$h = 22.20$ ft
$L_1 = 89.03$ ft,	$L_2 = 60.98$ ft
$\bar{x} = 90.00$ ft,	$\bar{z} = 11.25$ ft
$x_{cs} = -52.50$ ft,	$z_{cs} = -11.25$ ft
$\delta_0 = 30.02$ deg,	$S_{cs}/b = 22.5$ ft
$\Delta\tau_1 = 1.0$ deg,	$\Delta\tau_2 = 1.0$ deg
$m = 500$ slug/ft,	$\mathrm{m} = 40$ slug/ft
$g = 32.2$ ft/s^2,	$I_{yy} = 1.0 \times 10^6$ slug • ft^2/ft
$\omega_1 = 18$ rad/s,	$\zeta_1 = 0.02$

The engine parameters are

$\bar{A}_D = 0.1482$,	$\bar{A}_N = 6.3500$
$T_0 = 2000.0$ deg R,	$Ae/b = 8.88$ ft

Table 5 Stability and control derivatives

Symbol	Aerodynamics	Engine Thrust	Exhaust Gas	Total	Units[a]
		Stability derivatives			
$(X)_{M_\infty}$	−3541.7	1235.4	152.74	−2153.6	lb/ft
$(X)_\alpha$	−1318.5	884.45	74.581	−359.52	(lb/ft)/deg
$(X)_q$	3.7685	−0.067617	−0.0057017	3.6952	(lb/ft)/(deg/s)
$(X)_\eta$	−17.354	15.437	3.6713	1.7540	(lb/ft)/deg
$(X)_{\dot\eta}$	0.064907	0.0000	0.0000	0.064907	(lb/ft)/(deg/s)
$(Z)_{M_\infty}$	−8379.4	0.0000	−419.64	−8799.0	(lb/ft)
$(Z)_\alpha$	−3759.9	0.0000	−204.91	−3964.8	(lb/ft)/deg
$(Z)_q$	15.115	0.0000	0.015665	15.130	(lb/ft)/(deg/s)
$(Z)_\eta$	−43.867	0.0000	−2.7139	−46.581	(lb/ft)/deg
$(Z)_{\dot\eta}$	0.26033	0.0000	0.0000	0.26033	(lb/ft)/(deg/s)
$(M)_{M_\infty}$	−23219.9	13521.4	−847.976	−10546.5	lb
$(M)_\alpha$	64991.4	9680.38	−414.061	74257.7	lb/deg
$(M)_q$	−923.194	−0.740074	0.0316553	−923.902	lb/(deg/s)
$(M)_\eta$	1998.16	168.955	17.8631	2184.98	lb/deg
$(M)_{\dot\eta}$	−15.9548	0.00000	0.00000	−15.9548	lb/(deg/s)
$(Q)_{M_\infty}$	3265.5	0.0000	51.158	3316.7	lb
$(Q)_\alpha$	2145.1	0.0000	24.980	2170.1	lb/deg
$(Q)_q$	−16.574	0.0000	−0.0019097	−16.576	lb/(deg/s)
$(Q)_\eta$	37.439	0.0000	0.43598	37.875	lb/deg
$(Q)_{\dot\eta}$	−0.28641	0.0000	0.0000	−0.28641	lb/(deg/s)
		Control derivatives			
$(X)_\delta$	−979.07	0.0000	0.0000	−979.07	(lb/ft)/deg
$(X)_{A_D}$	0.0000	−75178.4	−6649.8	−81828.3	lb/ft
$(X)_{T_0}$	0.0000	6.1943	0.22297	6.4173	(lb/ft)/deg R
$(Z)_\delta$	−981.81	0.0000	0.0000	−981.81	(lb/ft)/deg
$(Z)_{A_D}$	0.0000	0.0000	18270.3	18270.3	lb/ft
$(Z)_{T_0}$	0.0000	0.0000	−0.61259	−0.61259	(lb/ft)/deg R
$(M)_\delta$	−40530.6	0.00000	0.00000	−40530.6	lb/deg
$(M)_{A_D}$	0.00000	−822832.9	36918.9	−785914.0	lb
$(M)_{T_0}$	0.00000	67.7973	−1.23788	66.5595	lb/deg R
$(Q)_\delta$	0.00000	0.00000	0.00000	0.00000	lb/deg
$(Q)_{A_D}$	0.00000	0.00000	−2227.30	−2227.30	lb
$(Q)_{T_0}$	0.00000	0.00000	0.0746804	0.0746804	lb/deg R

[a] Forces and Moments are per vehicle width in ft.

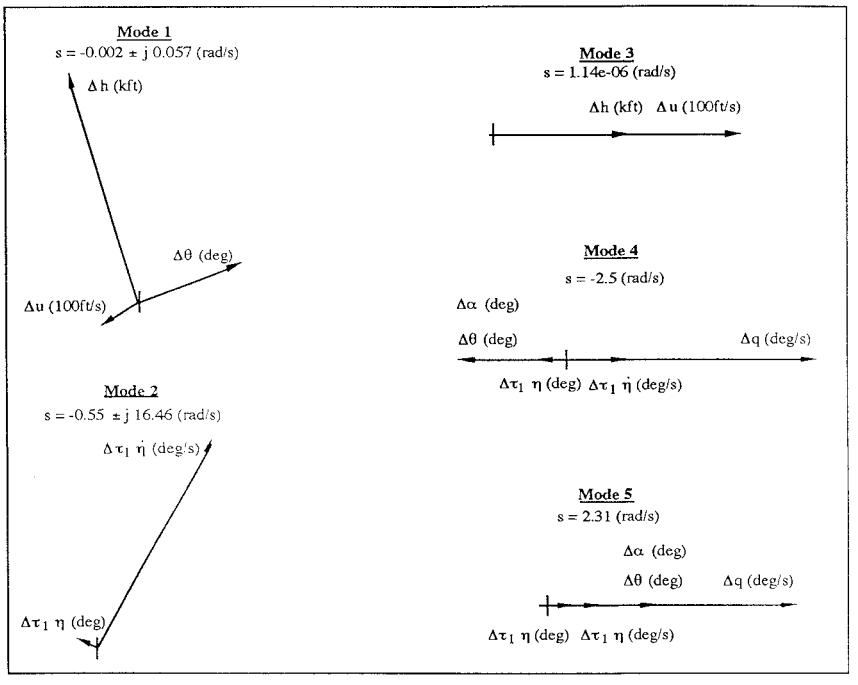

Fig. 6 Open-loop system modes and frequencies.

The flight condition (standard atmosphere at 85,000 ft) is given by

$$\alpha_0 = -2.00 \text{ deg}, \quad M_\infty = 8.0, \quad V_\infty = 7820.45 \text{ fps}$$
$$P_\infty = 44.95 \text{ psf} \quad T_\infty = 396.36 \text{ deg R}$$

For such a vehicle, the stability and control derivatives have been calculated and are tabulated in Table 5. (Again note that all variables are normalized per unit vehicle width.) The integrated stability derivatives for the vehicle are the sum of the contributions from the aerodynamics (A), the engine thrust (T), and the external exhaust plume (E).

From these results, note, for example, that in some cases the contributions from the engine-module thrust are as large as 50% of the associated aerodynamic effect, which is essentially the force on the fore-body. Also, the engine effects are destabilizing.

A modal analysis of the system (i.e., the eigenvalues and eigenvectors of the system) is shown in Fig. 6, where the units for the state vector have been converted to the following: [h (1000 ft), u (100 ft/s), α (deg), θ (deg), q (deg/s), $\Delta\tau_1\eta$ (deg), $\Delta\tau_1\dot{\eta}$ (rad/s)]^T. From the system eigenvectors, note that the system modes include a lightly damped oscillatory mode of low frequency, but unlike a conventional phugoid mode, this mode has significant height participation. Also, the vehicle exhibits an aeroelastic bending mode with a frequency of 16.5 rad/s, an unstable height mode, and a coupled pitch/bending mode with two real poles near ± 2.4 rad/s. The vehicle is therefore highly unstable in pitch, with significant pitch/bending interactions.

With the analytic expressions for the vehicle's stability derivatives and the use of literal expressions for the system poles and zeros from Ref. 14, the strong coupling between the vehicle's aerodynamics and propulsive forces become evident through further analysis of the dynamic characteristics of the vehicle. A 10% change in the vehicle's aerodynamic forces will produce a 34% change in the vehicle's short-period frequency, a 14% change in the elastic mode frequency, and a 50% change in the elastic mode damping. Just as significant, a 10% change in the vehicle's propulsive thrust characteristics will produce an 11% change in the vehicle's short-period frequency.

Conclusions

The flight dynamics of highly integrated hypersonic vehicles depend on the airframe's aerodynamic characteristics, engine thrust characteristics, and the integrated external nozzle. An integrated approach was developed for analyzing these dynamics, including defining new stability derivatives that include propulsive and aeroelastic effects. Analytical expressions were then developed for estimating all these stability derivatives, which account for aeropropulsive effects plus allow for the dynamic elastic deformation of the airframe. The numerical results for a generic hypersonic lifting body with SCRAMjet propulsion indicated that the engine module thrust characteristics increased the level of static instability, and in several cases, the propulsion system effects (engine module plus external nozzle) constitute over half of the numerical value of a particular stability derivative. This is not only true for the axial force derivatives, but for some of the moment derivatives as well. Furthermore, inspection of the control derivatives indicates that the engine controls (diffuser ratio and fuel flow) significantly affect the forces and moment on the airframe.

A modal analysis of the vehicle's dynamics further revealed that the study configuration is unstable in pitch and has strong airframe/engine/elastic coupling. The coupling effects were evident in the system eigenvectors (modeshapes). From these results, it is evident that both the aeropropulsive and aeroelastic effects contribute significantly to the overall dynamic character of the vehicle, and consequently an integrated modeling approach is required.

Acknowledgment

This research is supported by NASA's Langley Research Center under grant NAG-1-1341. Irene Gregory is the technical monitor.

References

[1]McRuer, D., "Design and Modeling Issues for Integrated Airframe/Propulsion Control of Hypersonic Flight Vehicles," *Proceedings of the American Control Conference*, Boston, MA, June 1991, pp. 729–735.

[2]Schmidt, D. K., Mamich, H., and Chavez, F., "Dynamics and Control of Hypersonic Vehicles—The Integration Challenge for the 1990's," AIAA Paper 91-5057, Dec. 1991.

[3]Schmidt, D. K., "Dynamics and Control of Hypersonic Aeropropulsive/Aeroelastic Vehicles," AIAA Paper 92-4326, Aug. 1992.

[4]Maughmer, M., Ozoroski, L., Straussfogel, D., and Long, L., "Validation of Engineering Methods for Predicting Hypersonic Vehicle Control Forces and Moments," AIAA Paper 91-2845, Aug. 1991.

[5]Gilbert, M. G., et al., "The Application of Active Controls Technology to a Generic Hypersonic Aircraft Configuration," NASA TM 1097, May 1990.

[6]Baranovsky, D. D., et al., "A Program of the Scramjet Design and Optimization," AIAA Paper 91-5073, Dec. 1991.

[7]Cheng, P. Y., "Aeroservoelastic Stabilization Techniques for Hypersonic Flight Vehicles," AIAA Paper 91-5057, Dec. 1991.

[8]*Aviation Week & Space Technology*, Oct. 29, 1990, p. 46.

[9]Chavez, F., and Schmidt, D. K., "An Integrated Analytical Aeropropulsive/Aeroelastic Model for the Dynamic Analysis of Hypersonic Vehicles," NASA ARC92-2, June 1992.

[10]Greenwood, D. T., *Principles of Dynamics*, Prentice-Hall, Englewood Cliffs, NJ, 1965.

[11]Anderson, J. D., *Modern Compressible Flow with Historic Perspective*, McGraw-Hill, New York, 1982.

[12]League, M., Farokhi, S., "Analysis of Pressure Distribution on Hypersonic Vehicles with Power Effects," AIAA Paper 91-2491, June 1991.

[13]Lees, L., "Hypersonic Flow," paper presented at the Fifth International Aeronautical Conference, Los Angeles, CA, 1955, pp. 241–276.

[14]Livneh, R., and Schmidt, D. K., "New Literal Approximations for the Longitudinal Dynamic Characteristics of Flexible Flight Vehicles," AIAA Paper 92-4411, Aug. 1992.